

# 2

## Thermal Properties of Solid and Molten Polymers

In addition to the mechanical and melt flow properties, thermodynamic data of polymers are necessary for optimizing various heating and cooling processes which occur in plastics processing operations.

In design work, the thermal properties are often required as functions of temperature and pressure [2]. As the measured data cannot always be predicted by physical relationships accurately enough, regression equations are used to fit the data for use in design calculations.

### ■ 2.1 Specific Volume

The volume-temperature relationship as a function of pressure is shown for a semicrystalline PP in Fig. 2.1 [1], and for an amorphous PS in Fig. 2.2 [1]. The  $p$ - $v$ - $T$  diagrams are needed in many applications; for example, to estimate the shrinkage of plastics parts in injection molding [19]. Data on  $p$ - $v$ - $T$  relationships for a number of polymers are presented in the VDMA-handbook [8].

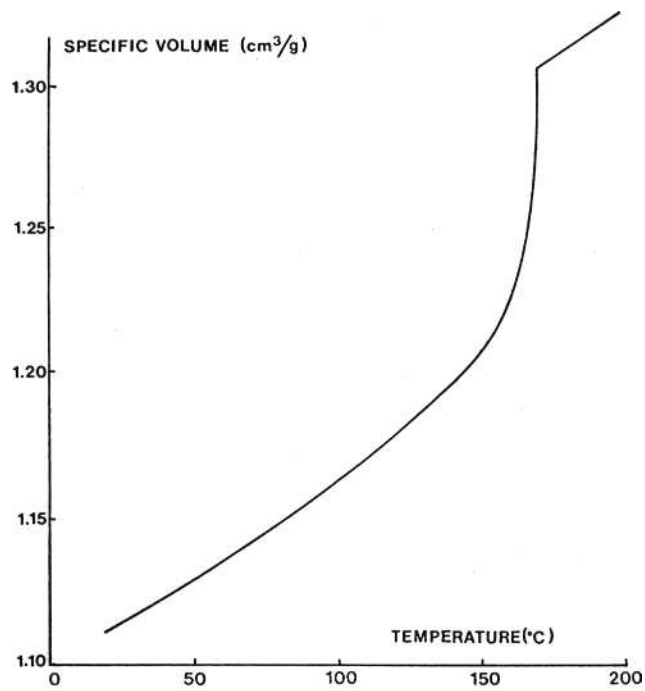


**Figure 2.1** Specific volume vs. temperature for a semicrystalline polymer (PP) [1]

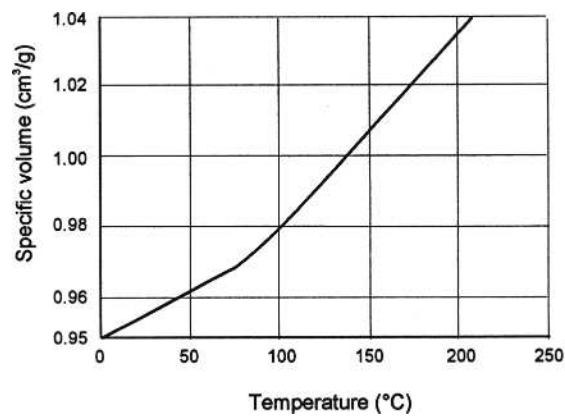


**Figure 2.2** Specific volume vs. temperature for an amorphous polymer (PS) [1]

According to the Spencer-Gilmore equation, which is similar to the van der Waals equation of state for real gases, the relationship between pressure  $p$ , specific volume  $v$ , and temperature  $T$  of a polymer can be written as

$$(v - b^*)(p + p^*) = \frac{RT}{W} \quad (2.1)$$

In this equation  $b^*$  is the specific individual volume of the macromolecule,  $p^*$  the cohesion pressure,  $W$  the molecular weight of the monomer, and  $R$  the universal gas constant [9].

The values  $p^*$  and  $b^*$  can be determined from  $p$ - $v$ - $T$  diagrams by means of regression analysis. Spencer and Gilmore and other workers evaluated these constants from measurements for the polymers listed in Table 2.1 [9, 18].

**Table 2.1** Constants for the Equation of State [9]

Material	$W$ g/mol	$p^*$ atm	$b^*$ cm <sup>3</sup> /g
PE-LD	28.1	3240	0.875
PP	41.0	1600	0.620
PS	104	1840	0.822
PC	56.1	3135	0.669
PA 610	111	10768	0.9064
PMMA	100	1840	0.822
PET	37.0	4275	0.574
PBT	113.2	2239	0.712

**Example:**

Following values are given for a PE-LD:

$$W = 28.1 \text{ g/mol}$$

$$b^* = 0.875 \text{ cm}^3/\text{g}$$

$$p^* = 3240 \text{ atm}$$

Calculate the specific volume at  $T = 190 \text{ }^\circ\text{C}$  and  $p = 1 \text{ bar}$

**Solution:**

Using Eq. 2.1 and the conversion factors to obtain the volume  $v$  in cm<sup>3</sup>/g, we obtain

$$v = \frac{10 \cdot 8.314 \cdot (273 + 190)}{28.1 \cdot 3240 \cdot 99 \cdot 1.013} + 0.875 = 1.292 \text{ cm}^3/\text{g}$$

The density  $\rho$  is the reciprocal value of specific volume so that

$$\rho = \frac{1}{v}$$

The  $p$ - $v$ - $T$  data can also be fitted by a polynomial of the form

$$v = A(0)_v + A(1)_v \cdot p + A(2)_v \cdot T + A(3)_v \cdot T \cdot p \quad (2.2)$$

### 3.2.6 True Viscosity

The true viscosity  $\eta_w$  is given by

$$\eta_w = \frac{\tau}{\dot{\gamma}_t} \quad (3.11)$$

In Fig. 3.11, the true and apparent viscosities are plotted as functions of the corresponding shear rates at different temperatures for polystyrene. As can be seen, the apparent viscosity function is a good approximation for engineering calculations.

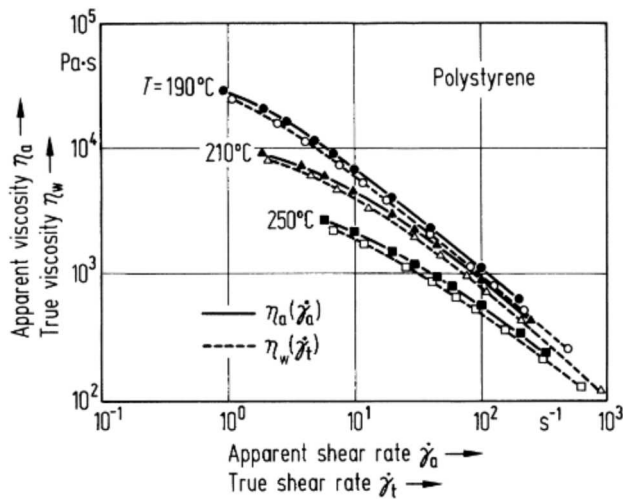


Figure 3.11 True and apparent viscosity functions of a polystyrene at different temperatures [4]

## 3.3 Rheological Models

Various fluid models have been developed to calculate the apparent shear viscosity  $\eta_a$  [2]. The following sections deal with an important few of these relationships, which are frequently used in design calculations.

### 3.3.1 Hyperbolic Function of Eyring and Prandtl

The relation between shear rate  $\dot{\gamma}_a$  and shear stress  $\tau$  according to the fluid model of Eyring [19] and Prandtl [20] can be written as

$$\dot{\gamma}_a = -C \sinh(\tau/A) \quad (3.12)$$

where  $C$  and  $A$  are temperature-dependent material constants.

The evaluation of the constants  $C$  and  $A$  for the flow curve of PE-LD at 190 °C in Fig. 3.12 leads to  $C = 4 \text{ s}^{-1}$  and  $A = 3 \cdot 10^4 \text{ N/m}^2$ . It can be seen from Fig. 3.12 that the hyperbolic function of Prandtl and Eyring holds well at low shear rates.

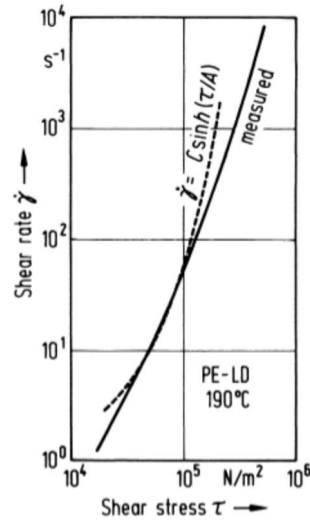


**Figure 3.12** Comparison between measurements and values calculated with Eq. 3.12 [2]

### 3.3.2 Power Law of Ostwald and de Waele

The power law of Ostwald [21] and de Waele [22] is easy to use, hence, it is widely employed in design work [5]. This relation can be expressed as

$$\dot{\gamma}_a = K \tau^n \quad (3.13)$$

or

$$\dot{\gamma}_a = K \left| \tau^{n-1} \right| \tau \quad (3.14)$$

where  $K$  denotes a factor of proportionality and  $n$  the power law exponent.

Another form of power law often used is

$$\tau_a = K_R \dot{\gamma}_a^{n_R} \quad (3.15)$$

or

$$\tau_a = K_R \left| \dot{\gamma}_a^{n_R-1} \right| \dot{\gamma}_a \quad (3.16)$$

In this case,  $n_R$  is the reciprocal of  $n$  and  $K_R = K^{-n_R}$ .

From Eq. 3.13, the exponent  $n$  can be expressed as

$$n = \frac{d \lg \dot{\gamma}_a}{d \lg \tau} \quad (3.17)$$

As shown in Fig. 3.13, in a double log-plot, the exponent  $n$  represents the local gradient of the curve  $\dot{\gamma}_a$  vs.  $\tau$ .

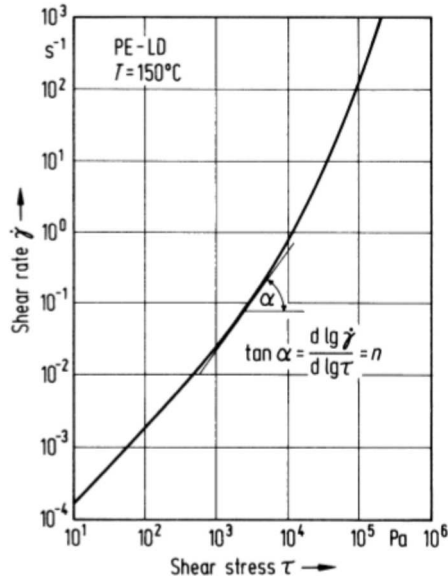


**Figure 3.13** Determination of the power law exponent  $n$  in the Eq. 3.13

Furthermore

$$\frac{1}{n} = \frac{d \lg \tau}{d \lg \dot{\gamma}_a} = \frac{d \lg \eta_a + d \lg \dot{\gamma}_a}{d \lg \dot{\gamma}_a} = \frac{d \lg \eta_a}{d \lg \dot{\gamma}_a} + 1 \quad (3.18)$$

The values of  $K$  and  $n$  determined from the flow curve of PE-LD at 190 °C, shown in Fig. 3.14, were found to be  $K = 1.06 \cdot 10^{-11}$  and  $n = 2.57$ .

As can be seen from Fig. 3.14, the power law fits the measured values much better than the hyperbolic function of Eyring [19] and Prandtl [20]. The deviation between the power law and experiment is a result of the assumption that the exponent  $n$  is constant throughout the range of shear rates considered, whereas  $n$  actually varies with the shear rate. The power law can be extended to consider the effect of temperature on viscosity as follows:

$$\eta_a = K_{OR} \cdot \exp(-\beta \cdot T) \cdot \dot{\gamma}_a^{n-1} \quad (3.19)$$

where  $K_{OR}$  = consistency index  
 $\beta$  = temperature coefficient  
 $T$  = temperature of melt

# 5

## Optical Properties of Solid Polymers

### ■ 5.1 Light Transmission

The intensity of light incident on the surface of a plastic is reduced as the light enters the plastic because some light is always reflected away from the surface. The intensity of light entering the plastic is further reduced as the light passes through the plastic since some light is absorbed, or scattered, by the plastic. The luminous transmittance is defined as the percentage of incident light that is transmitted through the plastic. For comparison purposes the exact test parameters are documented in ASTM D 1003. Some typical light transmission values for the most common optical plastics are presented in Table 5.1. Light transmission is a measurement of the transparency of a plastic.

**Table 5.1** Light Transmission or Luminous Transmittance of Some Common Optical Plastics

Material	Luminous transmittance D 1003
ABS	85
PC	89
PMMA	92
PMMA/PS	90
PS	88
SAN	88

### ■ 5.2 Haze

Haze is defined as the percentage of transmitted light which deviates from the incident light beam by more than 2.5 degrees. Its measurement is also defined by ASTM D 1003. Some typical haze values are presented in Table 5.2 for the most common optical plastics. Haze is a measure of the clarity of a plastic.

**Table 5.2** Haze of Some Common Optical Plastics

Material	Haze
ABS	10
PC	1–3
PMMA	1–8
PMMA/PS	2
PS	3
SAN	3

## ■ 5.3 Refractive Index

The refractive index  $n$  of an isotropic material is defined as the ratio of the speed of light in the material  $v$  to the speed of light in vacuum  $c$ , that is,

$$n = v/c$$

The speed of light in vacuum is 300,000 km/s. The refractive index decreases as the wavelength of the light increases. Therefore, the refractive index is measured and reported at a number of standard wavelengths, or atomic emission spectra (AES) lines, as indicated in Table 5.3.

**Table 5.3** Refractive Indices as Functions of Wavelength

AES line	Wavelength	PMMA	PS	PC
F	486 nm	1.497	1.607	1.593
D	589 nm	1.491	1.590	1.586
C	651 nm	1.489	1.584	1.576

The refractive index is usually measured using an Abbe refractometer according to ASTM D542. The Abbe refractometer also measures the dispersions, which is required for lens design. An extensive list of refractive indices is provided in Table 5.4. Since the speed of light in the polymer  $v$  is a function of the density, polymers which exhibit a range of densities also exhibit a range of refractive indices. Since density is a function of crystallinity, the refractive index is dependent on whether the polymer is amorphous or crystalline, and on its degree of crystallinity. Since density is also a function of temperature, decreasing as temperature increases, the refractive index also decreases with increasing temperature.



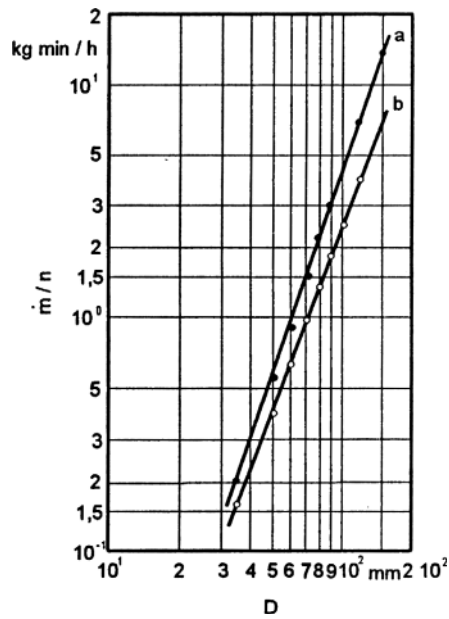


Figure 7.38 Empirical screw design data [11]

## ■ 7.3 Extrusion Dies

Extrusion dies can be designed by calculating shear rate, die pressure, and the residence time of the melt as functions of the flow path of melt in the die [6]. Of these quantities, the die pressure is the most important as the desired throughput cannot be attained if the die pressure does not match with the melt pressure. The interaction between screw and die is shown in Figs. 7.39 and 7.40.

Common shapes of flow channels occurring in extrusion dies are shown in Fig. 7.41. Detailed treatment of die design is presented in [1] and [17]. The following areas of application of extrusion dies serve as examples to illustrate the relationship between die geometry and processing parameters:

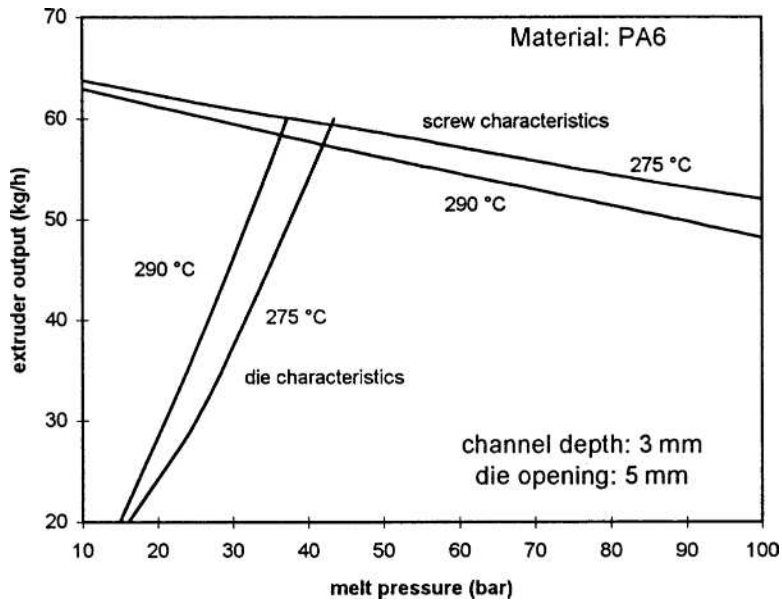


Figure 7.39 Effect of screw and die temperature

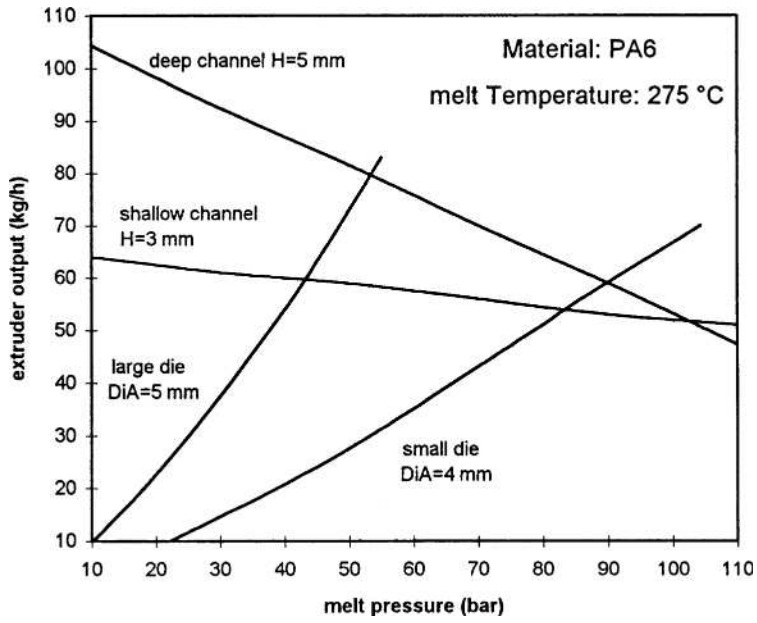


Figure 7.40 Effect of channel depth and die opening

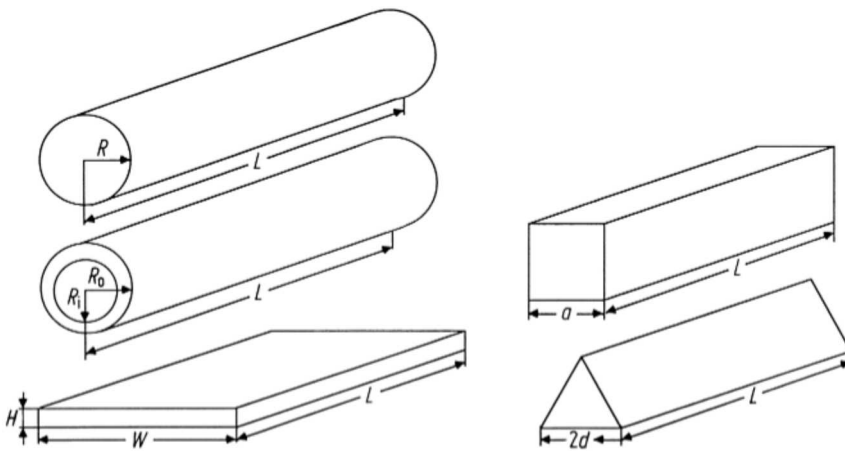


Figure 7.41 Common shapes of flow channels in extrusion dies [1]

### 7.3.1 Pipe Extrusion

The spider die shown in Fig. 7.42 is employed for making tubes and pipes and also for extruding a parison required to make a blow-molded article. It is also used in blown film processes.

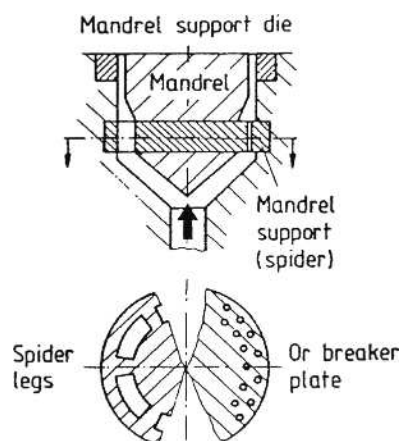


Figure 7.42 Mandrel support die with spider or break plate [17]

For a circular channel, the shear rate is given in Table 7.7. For an annulus, which represents the pipe cross-section, it is given by

$$\dot{\gamma}_{\text{annulus}} = \frac{6\dot{Q}}{\pi(R_o + R_i)(R_o - R_i)^2} \quad (7.28)$$

# Index

## A

absorption 100

## B

barrel screw 118  
Barr screw 112  
Biot number 174  
blown film 155  
Brinkman number, Br 174, 204  
bulk modulus K 11

## C

chemical resistance 101  
color 95  
comparative tracking index (CTI)  
  90  
composites 103  
compounding 167  
contact temperature 35  
cooling of channels 231  
cooling of melt 231  
  – crystalline polymers 231  
cooling time 234  
creep modulus 12  
creep rupture 14

## D

Deborah number 174  
design of mold 212  
dielectric strength 88

die swell 67  
diffusion coefficient 100  
dimensionless number 173  
drying temperatures 191

## E

elastomers 106  
enthalpy h 32  
extruder output 118  
extrusion cooling 170  
extrusion dies 145  
extrusion screws 112

## F

fatigue 15  
flammability 38  
fluid, non-Newtonian 45

## G

gates 202  
gloss 155

## H

heat deflection temperature (HDT)  
  36

**I**

impact strength 19  
injection molding 185  
– clamp force 204  
– mold 185  
– pressure 188  
– processing temperature 189  
– resin 191  
– runner system 220  
– screw 197

**L**

liquid-crystal polymers 104  
loss tangent 89

**M**

melt flow index (MFI) 63  
mold shrinkage 188

**N**

normal stress coefficient 65

**P**

permeability 99  
pipe extrusion 147

**R**

reinforced plastics 103  
relaxation modulus 14  
rheological models 51

**S**

shear compliance,  $J_e$  66  
sheet extrusion 161  
specific volume  $v$  26  
spider die 147  
surface resistivity 87

**T**

thermal conductivity 32  
thermoforming 163  
twin screws 114

**V**

velocity 44  
volume resistivity 87

**W**

weathering resistance 100